Heliyon 10 (2024) e36329

Contents lists available at ScienceDirect

Heliyon

journal homepage: www.cell.com/heliyon

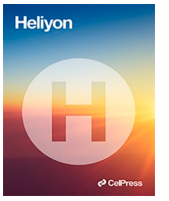

Research article

Reproductive and transcriptome characteristics of endometrium at the window of im-plantation in patients after fertility-sparing treatment of endometrial intraepithelial neoplasm or cancer

Penghui Feng [1], Duoduo Zhang [1], Jingran Zhen [**], Rong Chen [*]

Department of Obstetrics and Gynecology, National Clinical Research Center for Obstetric & Gynecologic Diseases, Peking Union Medical College Hospital, Chinese Academy of Medical Sciences & Peking Union Medical College, Beijing, 100730, China

ARTICLE INFO

Keywords:
Endometrial cancer
Fertility-sparing treatment
Endometrial receptivity
Window of implantation
Transcriptome

ABSTRACT

Background: Progestin therapy is an option for patients with endometrial carcinoma (EC) or endometrial intraepithelial neoplasm (EIN) who fit specific criteria of fertility-sparing treatment. However, the implantation rate remains low among females receiving in vitro fertilization (IVF) even after the complete reversal of endometrial lesions.

Methods: Here, ten patients with EC/EIN achieved complete regression (CR) in histology. Their relevant metabolic and IVF parameters were collected. An endometrial sampling at the window of implantation (WOI) and transcriptome analysis were conducted among them, and four healthy controls were analyzed to analyze endometrial receptivity.

Results: On average, it took ten patients five months to achieve CR after four curettage procedures. The interquartile range of endometrium thickness on trigger day was between 8.8 and 10.0 mm, while the range was 15.2–18.5 mm for controls. Five patients got pregnant after a frozen-embryo transfer. According to ERA analysis, the endometrial sampling at WOI showed pre-receptive status in four cases. In total, 1458 differential expression genes were identified, and 70 belonged to the ERA genes. ImmuneScore indicated decreased NK cells in the endometrium, affecting endometrial receptivity.

Conclusions: Even after EC/EIN reversal in histology, endometrial receptivity has already been compromised regarding altered WOI and immune microenvironment, leading to a low pregnancy rate.

1. Introduction

With 417,000 newly diagnosed cases in 2020, endometrial carcinoma (EC) is the sixth most prevalent cancer in women worldwide, particularly in developed countries [1]. Endometrioid adenocarcinoma is the most common histology, and atypical hyperplasia or endometrial intraepithelial neoplasm (EIN) is the precursor lesion of EC tumorigenesis [2]. Although total extra-fascial hysterectomy and bilateral salpingo-oophorectomy are the standard management for both conditions, conservative treatment is an option for patients who have not completed childbearing [3,4]. Estrogen promotes the proliferation of the endometrium, and progesterone counters

* Corresponding author.
** Corresponding author.
E-mail addresses: zhen_amy@126.com (J. Zhen), chenrongpumch@163.com (R. Chen).
[1] These authors contributed equally to this study.

https://doi.org/10.1016/j.heliyon.2024.e36329
Received 19 September 2023; Received in revised form 13 August 2024; Accepted 13 August 2024
Available online 17 August 2024

List of abbreviations

EC	endometrial carcinoma
EIN	endometrial intraepithelial neoplasm
IVF	in vitro fertilization
WOI	window of implantation
HESP	highly effective synthetic progesterone
CR	complete regression
ART	assisted reproductive technology
E2	estradiol
P	progesterone
MPA	medroxyprogesterone acetate
ICSI	intracytoplasmic sperm injection
ET	embryo transfer
HRT	hormone replacement therapy
DEGs	differentially expressed genes
FC	fold change
GO	Gene Ontology
KEGG	Kyoto Encyclopedia of Genes and Genomes
BP	biological process
CC	cellular component
MF	molecular function
GSVA	gene set variation analysis
PPI	protein-protein interaction
OGTT	oral glucose tolerance test
AMH	anti-mullerian hormone
FSH	follicle-stimulating hormone

this action. Thus, systematic treatment based on highly effective synthetic progesterone (HESP) is the core of fertility-sparing therapy [5], achieving a complete regression (CR) rate of 70.3 % in Grade 1 endometrial adenocarcinoma and 80.6 % in EIN [6,7].

Fertility is an urgent issue for these patients because the relapse rate after CR for progesterone therapy is 40–88 % [8,9]. Even with the help of assisted reproductive technology (ART), only 41.0 % of women with EIN and 34.8 % with EC can achieve pregnancy after the medical reversal of the lesion [6]. The compromised pregnancy rate could result from both the disease and the treatment procedure. The long-time appliance of HESP is depicted as detrimental to pregnancy [10]. Besides, the repeated curettage for endometrial evaluation over conservative care can lead to Asherman syndrome and harm fecundity [11]. These disadvantages possibly affect endometrial receptivity. Normal receptivity is attained approximately four to six days following ovulation, driven by sequential actions of estradiol (E2) and progesterone (P) and downstream molecular responses [12]. In this window of implantation (WOI), the blastocyst can attach to the endometrial epithelial cells and subsequently invade its stroma and vasculature. During this decidualizing process, endometrial transcriptomes are distinguished, and comercial arrays targeting receptivity have already been applied to guide embryo transfer [13]. In addition, there has been strong evidence that immune response mediate stromal and inflammatory regulators promote the opening of WOI [14]. However, few studies have focused on the endometrial functional changes in patients finished HESP reversal treatment. Rare cases reported the clinical characteristics in treating EC/EIN and receiving ART simultaneously, let alone the gene transcription patterns that accompany WOI opening.

We assume EC/EIN and the fertility-sparing therapy could leave a sequela on endometrial receptivity, responsible for the low pregnancy rate after the reversal of the endometrium lesion. Therefore, we conducted a clinical observation of an EC/EIN cohort that received HESP treatment and achieved CR (Pathological examination showed that all the diseased glands of endometrial atypical hyperplasia or cancer tissue had disappeared and were replaced by small flat cubic glands. Imaging examination showed no evidence of tumor in the thoracoabdominal and pelvic cavity). We aim to summarise their metabolic and endocrine profiles, pathology characteristics, and details relevant to ART so as to provide a whole landscape in the preservation and promotion of EC/EIN patients' fertility. Meanwhile, we try to illustrate the alteration of the endometrial transcriptome during WOI and the variation of the immune microenvironment from a bioinformatics perspective.

2. Materials and methods

2.1. Participants recruitment

Ten EC/EIN patients after fertility-sparing treatment (experimental group) and four women with childbearing history (control group) were prospectively recruited from 2020–01 to 2020–12. This study was approved by the Ethics Committee of Peking Union Medical College Hospital (IRB number: JS-3329), and written consent was obtained from all 14 participants. The inclusion criteria for

EC/EIN patients were: (1) younger than 40 years old; (2) a strong desire for fertility preservation; (3) well-differentiated (Grade 1) endometrioid adenocarcinoma or EIN confirmed by pathology; (4) lesions confined to the endometrium by magnetic resonance (MR); (5) no contraindication for HESP medication. The inclusion criteria for the control group were: (1) younger than 40 years old; (2) regular menses; (3) history of spontaneous pregnancy and vaginal delivery; (4) no history of curettage or other intrauterine operation.

2.2. Fertility-sparing treatment and assisted reproduction

The experimental group receives medication of HESP (Medroxyprogesterone acetate, MPA, 250–500 mg PO QD, Pfizer Italia Srl, or megestrol acetate, MA 320 mg PO QD, Guohai Pharma, Qingdao) as a conservative treatment for EC/EIN after evaluation for histology and metabolism status. Endometrial biopsy under hysteroscopy is repeated about every three months over the fertility-sparing process. Once the pathology demonstrates CR, patients will be referred to the ART center for evaluation, and further reproductive assessment and in vitro fertilization (IVF)/intracytoplasmic sperm injection (ICSI)-embryo transfer (ET) will be arranged according to the relevant indication. Clinical profiles related to the EC/EIN evaluation and treatment and the following IVF/ICSI outcomes are documented.

2.3. Endometrial sampling at WOI and ERA analysis

All participants from the experimental group or control group were given the standardized hormone replacement therapy (HRT) regimen applied orally for endometrial preparation for frozen thaw cycles. This consisted of daily administration of 4 mg of estradiol valerate (Progynova, Bayor, Germany) for 17–19 days, with co-treatment for the last five days with 30 mg of dydrogesterone (Duphaston, Abott, America). An endometrial biopsy and peripheral blood sample were collected on the day equivalent to embryo transfer, after five full days of progesterone administration on the morning of the sixth day (P+6), 1–3 h after administration of the morning dose of estradiol valerate and dydrogesterone. The sample from each biopsy was stored and sent for endometrial receptivity array (ERA) testing (Igenomix, Valencia, Spain) according to the protocol provided by Igenomix. ERA is a diagnostic tool used in ART to evaluate the receptivity of the endometrium, the lining of the uterus, to embryo implantation. The sampling method involves taking a small biopsy of the endometrial tissue, usually during the mid-luteal phase of the menstrual cycle, when the endometrium is expected to be most receptive. The main aim of the ERA testing is to determine the optimal WOI for an individual woman. By analyzing the gene expression profile of the endometrial biopsy, the ERA can identify whether the endometrium is receptive or not at the time of sampling. This helps to pinpoint the precise timing when the endometrium is ready for embryo implantation.

2.4. Transcriptome sequencing and differential expression analysis

Endometrial sampling was carried out by endometrial brush sampler and then tranferred into TRIzol reagent. DNA digestion was perfomed after RNA extraction by DNaseI. RNA quality was confirmed by examining A260/A280 with Nanodrop. RNA Integrity was determined by 1.5 % agarose gel electrophoresis. Qualified RNAs were quantified using Qubit 3.0 and used for cDNA library construction and RNA bulk sequencing. The original sequencing data of all participants were obtained by Illumina Hiseq sequencing in FASTQ format, which was further processed by Trimmomatic; low-quality reads were discarded and the reads contaminated with adaptor sequences were trimmed. After alignment, assembly, and annotation, gene expression profiles were finally calculated and quantified as reads per kilobase per million reads when mapping to the corresponding reference genomes. Based on the above analysis, the differentially expressed genes (DEGs) were screened out once meeting the following criteria: $\log2 |\text{fold change (FC)}| > 1$ and P value < 0.05, which was adjusted by false discovery rate (FDR) when performing multiple hypothesis testing.

2.5. Functional enrichment analysis of target genes

DEGs were imported for clustering, which depended on their expression level using the pheatmap package (https://CRAN.R-project.org/package=pheatmap). Another R package, clusterProfiler [15], was adopted to determine and visualize the potential functions of the identified genes for Gene Ontology (GO) and Kyoto Encyclopedia of Genes and Genomes (KEGG) pathway enrichment. As concerned, GO analysis, an internationally standardized classification system of gene function, provides a dynamically updated and controlled vocabulary to comprehensively describe the properties of target genes and gene products, which consist of three ontologies (biological process, molecular function, and cellular component). As for KEGG, it converges genome information and functional information by integrating the metabolic pathways database, stratified classification database, and gene database. In this study, a P value < 0.05 was considered significant.

2.6. GSVA procedures

Gene set variation analysis (GSVA) was applied here using the GSVA package [16], which incorporates the implementation of four single-sample gene set enrichment methods: concretely, zscore, plage, ssGSEA, and GSVA. As a non-parametric, unsupervised method of gene set enrichment, it enables pathway-centric analyses of molecular data by converting the expression matrix of genes among samples into the expression profiles of gene sets to estimate the enrichment of different pathways. In the present study, the genes of each sample were deposited for their cumulative density function. Data was finally exhibited, as shown in the heatmap.

2.7. Protein-protein interaction (PPI) establishment

To evaluate the underlying interaction of the target genes, the PPI network was constructed based on the STRING database (https://string-db.org/) [17]. The merged genes were input for the further calculation to clarify their interactive relation among genes with the minimum required interaction score >0.7 (high confidence). Node information was further imported into GEPHI software to display the connection degree of all involved nodes or genes.

2.8. Immune infiltration evaluation by CIBERSORT and ESTIMATE algorithm

The algorithm of Estimation of Stromal and Immune cells in Malignant Tumor Tissues Using Expression Data (ESTIMATE, https://bioinformatics.mdanderson.org/estimate) is well in assessing the scores for tumor purity, the level of stromal cells, and the infiltration level of immune cells in tumor tissues based on expression data [18]. At the same time, CIBERSORT was introduced into this study to estimate the abundances of member cell types in a mixed cell population using gene expression data (The CIBERSORT algorithm is a computational method used to deconvolute bulk RNA sequencing data. It enables the identification and quantification of different cell types within a mixed cell population by analyzing gene expression profiles. CIBERSORT employs a set of reference gene expression signatures from known cell types to estimate the relative proportions of each cell type in the sample. This approach is particularly valuable in contexts where understanding the cellular composition of a tissue is essential, such as in cancer research, immunology, and studies of complex tissues, allowing researchers to gain insights into cellular heterogeneity and its implications for health and disease). In this study, ESTIMATE and CIBERSORT algorithms were integrated to analyze the cell composition in the tumor microenvironment of endometrial cancer. Expression profiles of all samples were processed and estimated by ESTIMATE and CIBERSORT algorithms, and the DEGs were identified by StromalScore and ImmuneScore, defined as sDEGs and iDEGs, respectively. Moreover, the incorporated DEGs were selected. DEGs were identified according to the limma package of R software [19]. DEGs between groups with high or low scores needed to satisfy the following criteria: log2 |fold change (FC)| $>$ 1 and P value $<$ 0.05.

3. Results

3.1. Clinical characteristics of all involved participants

Overall, 10 EC/EIN patients and four controls were recruited. The general characteristics of the experimental group are illustrated in Table 1. None of them had a gravid history. The age of menarche fell within the normal range, but six of them experienced an oligomenorrhea or amenorrhea (cycles>35 days) later. In terms of metabolism, all patients received an evaluation of HbA1c, and eight underwent a 2-h oral glucose tolerance test (OGTT) and its synchronous serum insulin (INS) measurement. The HbA1c and OGTT found no case with diabetes or impaired glucose tolerance, but INS hint that the insulin secretion had been postponed, and the homeostasis model assessment of insulin resistance (HOMA-IR>2.5–2.8) was abnormally high in Case 5, which indicated a status of insulin resistance [20]. The comprehensive metabolic panel showed that Cases 3, 5, and 9 have hypertriglyceridemia, and Case 5 had hypercholesteremia and hyperuricemia.

The endometrium pathologies were diagnosed as EC (endometrial endometrioid cancer) in six patients, while the rest were EIN (Table 2). In this study, all cases involved were determined as FIGO 1A or earlier of endometrial lesions. The histochemistry further proved that none had mismatch repair deficiency or *P53* mutation, and estrogen and progesterone receptors were positive for neoplasm tissues from each case. All patients had serum CA125 within the normal range. The MR revealed only Cases 8 and 10 with suspicious superficial invasion in the uterine junction zone, and the other eight cases were detected as no positive signs at the imaging level. Among these patients, eighty percent lost more or less weight before and after treatment. It took a median time of five months (interquartile range 3–8 months) for histology to meet CR for the first time. Over the fertility preserving medication, patients experienced curettage four times in medium, and the interquartile range was between 3 and 5 times. The ERA sampling at WOI showed pre-receptive status (before P+4) of the endometrium of Cases 3, 5, 9, and 10, while the other six patients and four controls were all shown as receptive status.

3.2. ART reproductive outcome of EC/EIN patients

After the accomplishment of EC/EIN treatment and endometrium sampling, ART cycles were initiated. Only six patients were under 35 years old at the time of ART, but all patients had antral follicle count (AFC)≥8 and anti-mullerian hormone (AMH) > 1.5 ng/mL. Among these ten participants, ERA analysis indicated that four patients' WOI status (Cases 3, 5, 9, and 10) were confirmed to be pre-receptive, and therefore, they received individualized embryo transplantation strategies (Table 3). Four patients used the agonist long protocol for ovarian stimulation, and six were arranged for the antagonist protocol (In ART, the agonist long protocol and antagonist protocol are used to control ovarian stimulation and prevent premature ovulation during IVF. The agonist-long protocol involves administering GnRH agonists starting in the luteal phase to first cause an initial surge and then suppress gonadotropin release, followed by gonadotropins for ovarian stimulation until eggs are retrieved. In contrast, the antagonist protocol begins in the follicular phase with gonadotropins for ovarian stimulation, introducing GnRH antagonists mid-cycle to immediately suppress LH and FSH without an initial surge, continuing until egg retrieval. The former is typically longer with potentially more side effects due to prolonged suppression, while the latter is shorter and offers greater flexibility) (Table 4). The initiation dosage of follicle-stimulating hormone (FSH) ranged between 150 and 300 U. Patients received frozen-thawed embryo transfer by HRT guided by ERA. The interquartile range of

Table 1
General reproductive and metabolic characteristics of patients.

Case	Gravidity	Age of menarche (years old)	Duration of menses (days)	Menstrual cycles (days)	Dysmenorrhea (Visual analogue scale score)	HbA1c (%)	OGTT (0 h-1h–2h)		HOMA-IR	Comprehensive metabolic panel
							Glu (mmol/L)	INS (μIU/mL)		
1	0	10	7	90	0	5.1	not available	not available	not available	NAD
2	0	13	10	360	3	5.0	4.2-7.5-4.9	5-109-81	0.93	NAD
3	0	12	7	180	0	5.1	not available	not available	not available	hypertriglyceridemia
4	0	14	14	60	2	5.1	4.3-5.5-5.5	8-112-107	1.53	NAD
5	0	10	7	120	1	5.9	5.1-8.5-7.0	19-152-219	4.31	hypertriglyceridemia hypercholesteremia hyperuricemia
6	0	14	5	30	2	4.8	4.6-7.7-5.2	2.9-157-98	0.59	NAD
7	0	13	7	30	1	5.0	4.9–7.7-4.6	8-103-60	1.74	NAD
8	0	13	7	50	7	5.2	4.4-10.8-5.4	6-155-73	1.17	NAD
9	0	14	8	29	1	5.1	4.9–7.3-5.0	6-107-43	1.31	hypertriglyceridemia
10	0	13	7	30	4	5.7	4.9–6.2-5.2	4-120-68	0.87	NAD

Notes: Glu, serum glucose level; HbA1c, glycosylated hemoglobin A1c; HOMA-IR, homeostasis model assessment of insulin resistance(normal reference <2.5–2.8); INS, serum insulin level; NAD, nothing abnormal detected; OGTT, oral glucose tolerance test.

Table 2
Information relevant to conservative management of endometrial lesions.

Case	Pathology	Uterine junction zone on MR	CA125 (U/mL)	Mismatch repair deficiency	Immunohistochemistry				BMI before treatment (kg/m^2)	BMI after treatment (kg/m^2)	Percentage of weight loss (%)	Medical management	Dosage	Total times of curettage	Time spent for reaching complete remission (months)
					p53	ER	PR	Ki67 (%)							
1	EIN	NAD	11.9	Neg	WT	+	+	60	27.06	25.10	9.23	MA	320 mg po QD	6	3
2	EIN	NAD	9.65	Neg	WT	+	+	10	22.66	23.04	0.00	MPA	250 mg po QD	3	4
3	EC	NAD	7.6	Neg	WT	+	+	30	28.04	24.06	12.86	MPA	500 mg po QD	2	3
4	EC	NAD	130	Neg	WT	+	+	40	33.20	21.51	35.29	MPA	500 mg po QD	3	7
5	EIN	NAD	18.9	Neg	WT	+	+	20	32.02	26.03	18.67	MA	320 mg po QD	2	4
6	EC	NAD	10	Neg	WT	+	+	5	23.88	24.22	0.00	MA	320 mg po QD	3	8
7	EC	NAD	16.1	Neg	WT	+	+	20	20.45	20.14	3.64	MA	320 mg po QD	4	3
8	EC	superficial invasion	9.7	Neg	WT	+	+	20	32.42	25.06	22.89	MA	320 mg po QD	5	12
9	EIN	NAD	7.8	Neg	WT	+	+	20	23.15	20.32	11.67	MPA	500 mg po QD	4	6
10	EC	superficial invasion	11.4	Neg	WT	+	+	20	17.92	17.03	2.83	MA	320 mg po QD	5	12

Notes: BMI, body mass index; EC, endometrial cancer; EIN, endometrial intraepithelial neoplasm; ER, estrogen receptor; GnRHa, gonadotropin-releasing hormone agonist; im, intramuscular; MA, megestrol acetate; MPA, medroxyprogesterone acetate; MR, magnetic resonance; NAD, nothing abnormal detected; po, peroral; PR, progesterone receptor; QD, per day; QM, per month; WT, wild type.

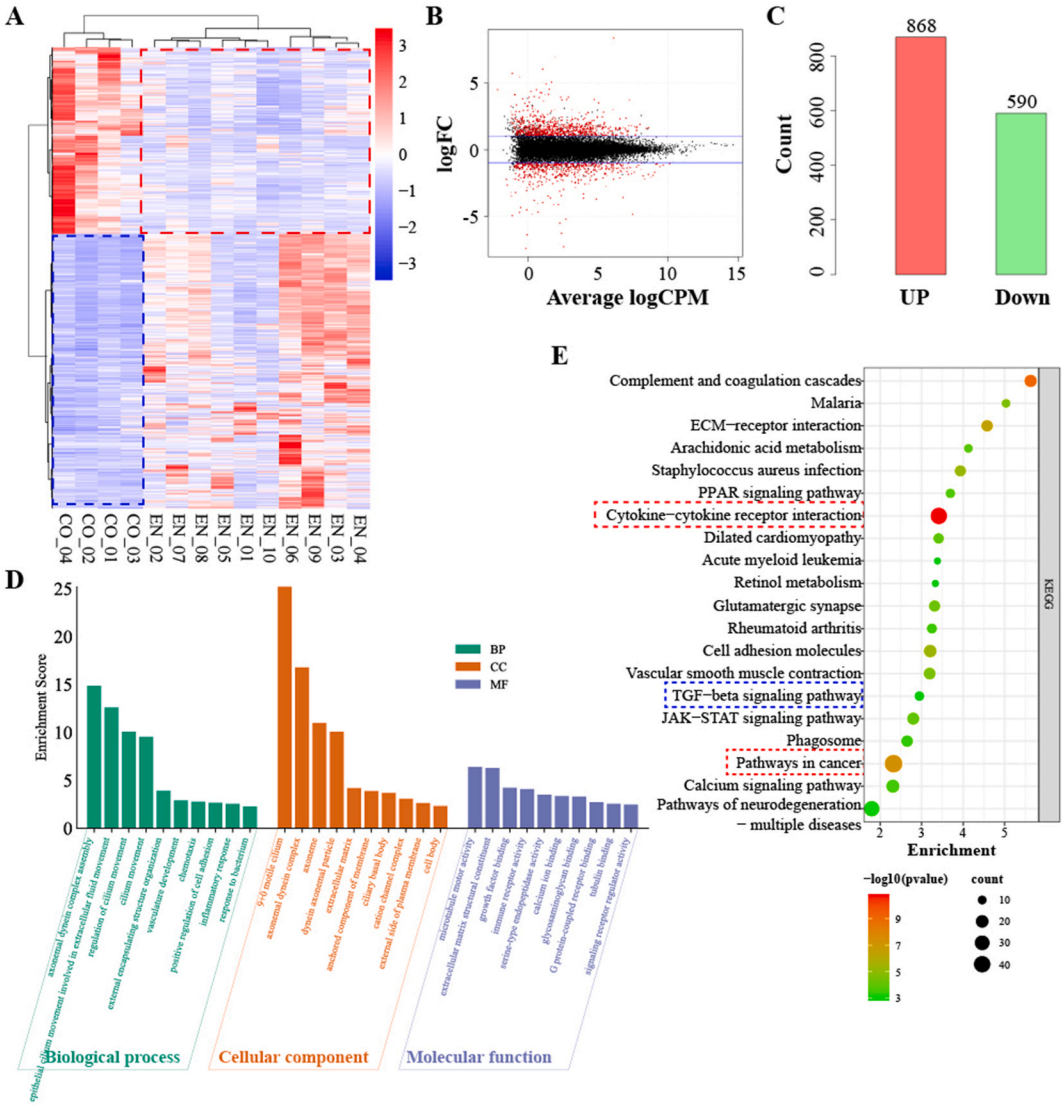

Fig. 1. Identification and functional enrichment of DEGs. **A.** The heatmap of the DEGs between the control and EC/EIN groups by hierarchical clustering and different colors represents the trend of gene expression in different tissues. **B.** M-versus-A plot of DEGs was constructed. The horizontal axis refers to the average log2 counts per million, and the vertical axis is log-fold-changes between each pair of RNA samples. **C.** Statistics of the number of up-regulated or down-regulated DEGs. **D.** Top enriched terms of the biological process (BP), cellular component (CC), and molecular function (MF) of the 1458 DEGs were clustered from GO enrichment. **E.** Annotation of the DEGs was selected to demonstrate their primary biological actions in the KEGG pathway by the KEGG mapper. (For interpretation of the references to color in this figure legend, the reader is referred to the Web version of this article.)

endometrium thickness on trigger day was between 8.8 and 10.0 mm, while the range was 15.2–18.5 mm for four controls. The interquartile number of eggs harvested was between 6 and 10. Everyone but Cases 4 & 5 was transferred with two embryos, and five patients (Cases 1, 2, 3, 4 & 6) became pregnant with a singleton. Cases 1 & 2 have given birth to healthy babies, while Cases 3, 4 & 6 were still in their ongoing pregnancy. Besides, half of them had miscarriages.

3.3. *Determination of DEGs and function analysis*

In the present study, we initially quantified the gene expression of the endometrium sampling at WOI between EC/EIN patients and healthy participants. The results demonstrated that the endometrial tissues exhibited different gene expression patterns between the two groups, and there were about, among all the DEGs, 868 genes were up-regulated and 590 down-regulated (Fig. 1 A, B, and C). It's worth noting that these genes were mainly involved in chemotaxis, inflammatory response, positive regulation of cell adhesion, and vasculature development in terms of their biological functions, as shown in Fig. 1 D. Besides, similar findings were also confirmed

Table 3
Laboratory examinations before entering IVF/ICSI cycle.

Case	Age at IVF/ICSI	AFC*	AMH* (ng/mL)	FSH* (IU/L)	LH* (IU/L)	E2* (pg/mL)	P* (ng/mL)	T* (ng/mL)	EM* (mm)	Hysterosalpingography	Endometrial receptivity analysis#	Thyroid function
1	34	35	10.81	5.93	6.18	26	1.1	0.44	4.4	normal patency	R	NAD
2	27	8	2.42	8.12	6.31	47	0.5	0.41	4.7	normal patency	R	NAD
3	29	13	1.56	6.14	3.77	35	0.1	0.57	4.8	normal patency	PRE	NAD
4	28	28	6.55	6.02	5.26	27	0.7	0.37	4.8	normal patency	R	NAD
5	39	22	2.43	6.52	6.05	25	0.7	0.5	9.1	normal patency	PRE	subclinical hypothyroidism
6	27	32	5.11	7.51	1.73	24	0.8	0.46	4.5	normal patency	R	NAD
7	37	11	1.53	7.77	2.28	68	1	0.37	3.7	normal patency	R	NAD
8	37	18	4.08	9.28	2.61	33	0.6	0.2	2.3	ipsilateral Interstitial obstruction	R	NAD
9	31	17	3.66	6.86	5.14	44	0.5	0.33	3.7	bilateral Interstitial obstruction	PRE	subclinical hypothyroidism
10	35	13	2.21	12.56	4.38	35	1.3	0.24	4.6	normal patency	PRE	NAD

Notes: *These tests were done on cycle day 2–5.
#Tested by ERA (Igenomix, Valencia, Spain), and the results were shown as PRO, proliferative; PRE, pre-receptive; R, receptive; POST, post-receptive.
AFC, antral follicle count; AMH, anti-mullerian hormone; E2; serum estradiol level; EM, endometrium thickness; FSH, follicle-stimulating hormone; ICSI, intracytoplasmic sperm injection; IVF, in-vitro fertilization; LH, luteinizing hormone; NAD, nothing abnormal detected; P; serum progesterone level; T, total serum testosterone level.

Table 4
Parameters and outcomes of IVF/ICSI treatment.

Case	Protocol	Initiation dosage (U)	Total gonadotropin (U)	Time spent on ovarian stimulation	E2* (pg/mL)	P* (ng/mL)	EM* (mm)	Oocytes retrieved	Fertilization	Embryos on Day 3	Good quality embryos	Blastocysts	Embryo transferred	Clinical pregnancy
1	Agonist long	150	1687.5	10	1661	0.3	9.6	10	ICSI	10	1	3	2	Singleton
2	Antagonist	225	2737.5	12	1760	0.97	8.2	6	IVF	6	1	3	2	Singleton
3	Agonist long	300	3525	10	1184	1	6.4	10	IVF	9	0	0	2	Singleton
4	Antagonist	225	1500	11	7330	0.82	10	20	ICSI	20	11	14	1	Singleton
5	Antagonist	300	2587.5	11	5257	1.61	13	8	ICSI	8	2	4	1	Not pregnant
6	Antagonist	150	1275	10	2035	1.02	11	7	IVF	7	3	6	2	Singleton
7	Agonist long	300	4725	14	1612	1.36	8.8	5	IVF	2	0	0	2	Not pregnant
8	Antagonist	300	2475	9	3679	0.98	14	8	IVF	6	0	4	2	Not pregnant
9	Antagonist	225	2587.5	10	1457	0.86	10	6	IVF	5	1	1	2	Not pregnant
10	Agonist long	300	3600	11	2287	1.86	8.7	5	IVF	2	0	0	2	Not pregnant

Notes: *These tests were done on trigger day. E2; serum estradiol level; EM, endometrium thickness; ICSI, intracytoplasmic sperm injection; IVF, in-vitro fertilization; P; serum progesterone level.

when they were annotated in KEGG pathways, that they were associated with cytokine-cytokine receptor interaction, extracellular matrix (ECM)-receptor interaction, TGF-β signaling pathway, and pathways in cancer (Fig. 1 E). These results suggested that immune regulation might have been altered in the EC/EIN group after CR and compromised the receptivity competence of endometrium.

3.4. Identification of ERA-related DEGs

Considering the above findings, we further explored the endometrial receptivity-related DEGs by comparing the DEGs and the reported 238 ERA genes (Fig. 2A). As concerned, the ERA functioned by analyzing the expression of 238 genes related to the implantation window and, therefore realizing individual WOI-guided embryo transfer to achieve accurate implantation [21,22]. Some research has proved that the embryo implantation rate was significantly improved after ERA detection and adjustment of implantation time, even for patients with recurrent implantation failure [23]. Here, ERA-related DEGs derived from both the DEGs and published 238 ERA genes were intersected, and eventually, 70 genes were acquired, of which 59 were down-regulated genes, and 11 were up-regulated genes overlapped with these ERA genes, as shown in the Upset plot (Fig. 2B). Subsequently, we further explored the potential roles of these genes. The expression matrix was redefined by them, followed by functional enrichment analysis performed by the GSVA algorithm. The TGF-β signaling, ECM receptor interaction, and neuroactive ligand-receptor interaction pathways were significantly changed between the two groups, according to GSVA. Intriguingly, the TGF-β signaling and ECM receptor interaction pathways had much to do with the characteristics of immune and receptivity in the endometrium, and the progression of endometrial cancer may account for their differences (Fig. 2C).

3.5. Immune infiltration estimation based on estimate score

Given that the differences in gene expression patterns in endometrial samples between the EC/EIN patients and healthy controls hint the altered immune regulation may be responsible for impaired endometrial receptivity, we ulteriorly estimate the abundance of immune cells and stromal cells in endometrial tissues, which were quantified by CIBERSORT algorithms. In this study, the estimated scores were divided into immune and stromal scores. Correspondingly, the higher the scores, the greater the proportion of cells. As observed, samples were remarkably distinguished between groups in aspects of the ImmuneScores and StromalScores (Fig. 3A and B). Consequently, 360 DEGs were defined by the StromalScores, regarded as sDEGs, and 402 DEGs were identified as iDEGs by the ImmuneSores. In total, 138 genes were down-regulated, and the rest of the genes were highly expressed (Fig. 3C). Based on the iDEGs

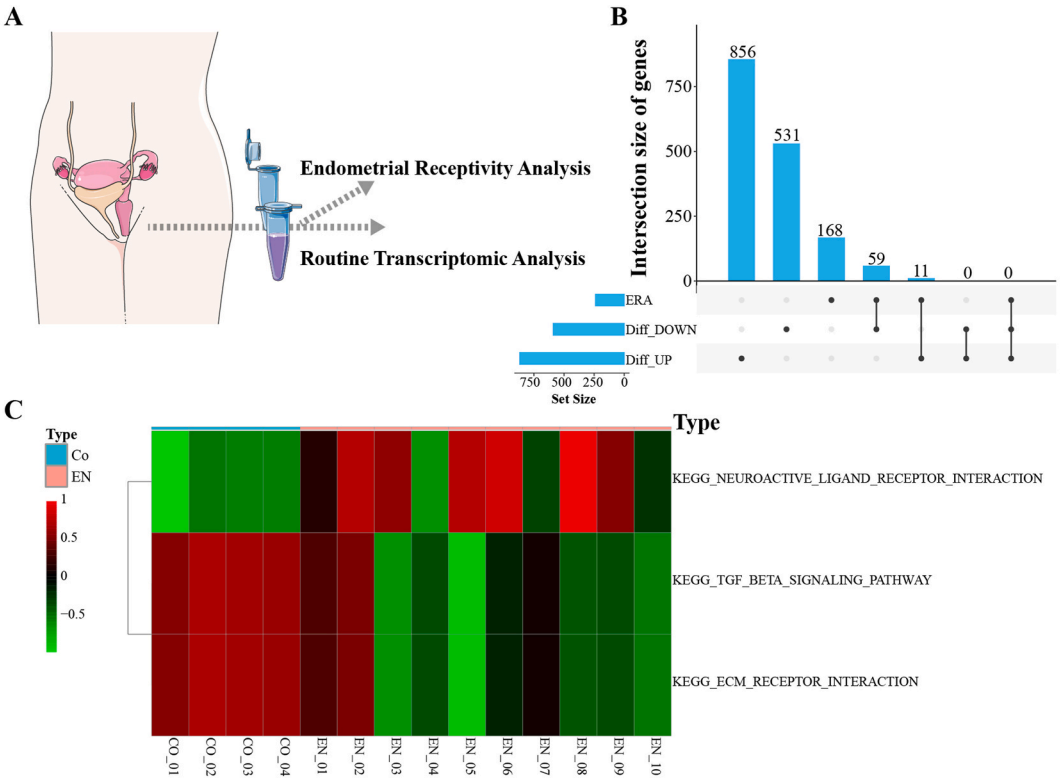

Fig. 2. Determination of ERA-related DEGs and GSVA analysis. **A.** Schematic diagram of routine transcriptomic analysis and ERA-related DEGs screening. **B.** The intersection of up-regulated or down-regulated DEGs between the control and EC/EIN groups and 237 ERA-related genes. Y-axis represents the number of merged genes. **C.** Gene set variation analysis based on gene expression matrix of the identified 70 ERA-related DEGs.

and sDEGs, GO analysis manifested that they were engaged in immune regulation, as most enriched pathways were closely related to immune cells migration and chemotaxis in the biological process. In terms of molecular function, these genes prevailingly enrolled in cytokine or immune receptor activity and immunoglobulin or chemokine binding, as shown in Fig. 3D. Similarly, KEGG annotation also indicated that these genes mainly functioned in the chemokine signaling pathway and cytokine-cytokine interaction. The observations confirmed the suspicions that immune modulation was bound up with receptivity variation during tumorigenesis of the endometrium.

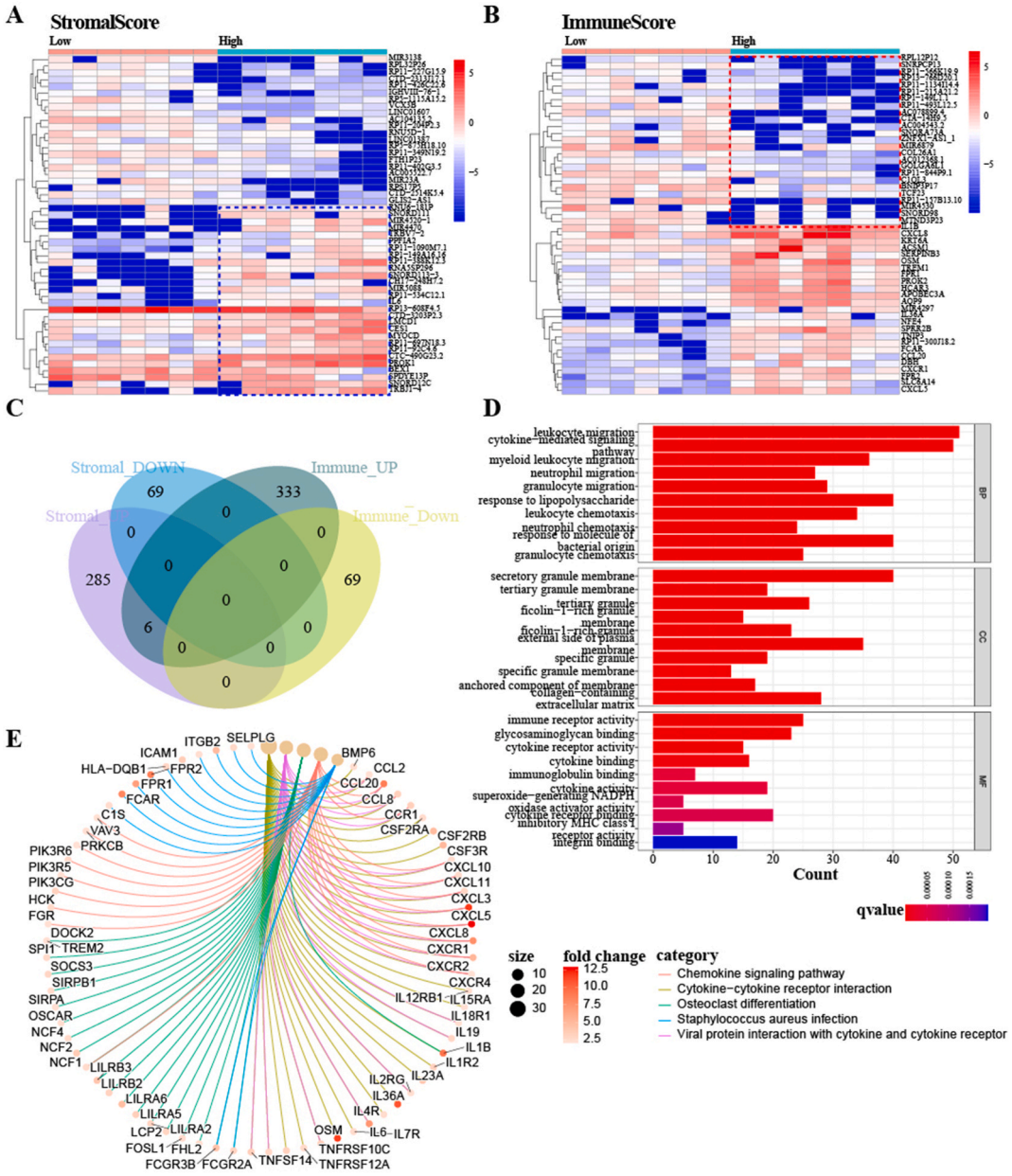

Fig. 3. Screening of tumor microenvironment-related genes based on Estimate scores and functional enrichment analysis. **A.** Top 50 ImmuneScore-based DEGs (iDEGs) based on CIBERSORT algorithms. Heatmap for DEGs generated by comparison of the high score group vs. the low score group in ImmuneScore. Row name of heatmap is the gene name, and column name is the ID of samples which not shown in plot. The relative expression level of these differential genes were calculated as fold-change value after log2 transformation and these differences were illustrated by changes in the color of the grid, where red represented high expression and blue represented low expression.**B.** Heatmap of top 50 StromalScore-based DEGs (sDEGs). **C.** Intersected genes of iDEGs and sDEGs. **D, E.** GO enrichment analysis and KEGG pathways of all iDEGs and sDEGs involved, respectively. Fold-change after log2 transformation was regarded as the gene relative expression level. Size represented the number of involved genes in the corresponding pathway. (For interpretation of the references to color in this figure legend, the reader is referred to the Web version of this article.)

3.6. Hub genes related to immune infiltration and endometrial receptivity

Furthermore, based on the confidence score, we established the protein-protein interaction (PPI) network to illustrate the interactive relationship among all involved iDEGs and sDEGs. All protein interaction data were weighted and integrated, and a reliable value was calculated (Fig. 4A). As a result, 200 crucial genes were identified, and their adjacent node enumeration was displayed, as presented in Fig. 4B. To determine the hub genes that were associated with immune infiltration and endometrial receptivity, we gathered the analytical results from differential expression analysis, PPI, and ERA-related genes, and whereafter, 10 hub genes were ultimately figured out, including *TIMP3*, *DPP4*, *THBD*, *LMOD1*, *HAND2*, *ADAMTS1*, *MYL9*, *ACTA2*, *CDA*, and *CES1* (Fig. 4C). In order to reveal the potential interaction of the 10 hub genes and the implicated immune cells, CIBERSORT was utilized here to evaluate the robust enumeration of immune cell subsets from endometrial tissues by deconvolution algorithm based on linear support vector regression. As shown, 13 major types of cell subsets in each sample were quantified and displayed in the stack bar chart, and B memory and $CD4^+$ T memory resting were highly enriched in the EC/EIN group ($P < 0.05$). Conversely, the resting and activated NK cells were primarily involved in the healthy group (Fig. 4D). Moreover, we clarified the correlation of the expression of these cell subsets as suggested in Fig. 4E; it was observed that the activated NK was positively correlated with the resting mast cells. Besides, the B memory cells exhibited inversed correlation with the M0 macrophages, resting mast cells, activated or resting NK cells, monocytes, and $CD8^+$ T

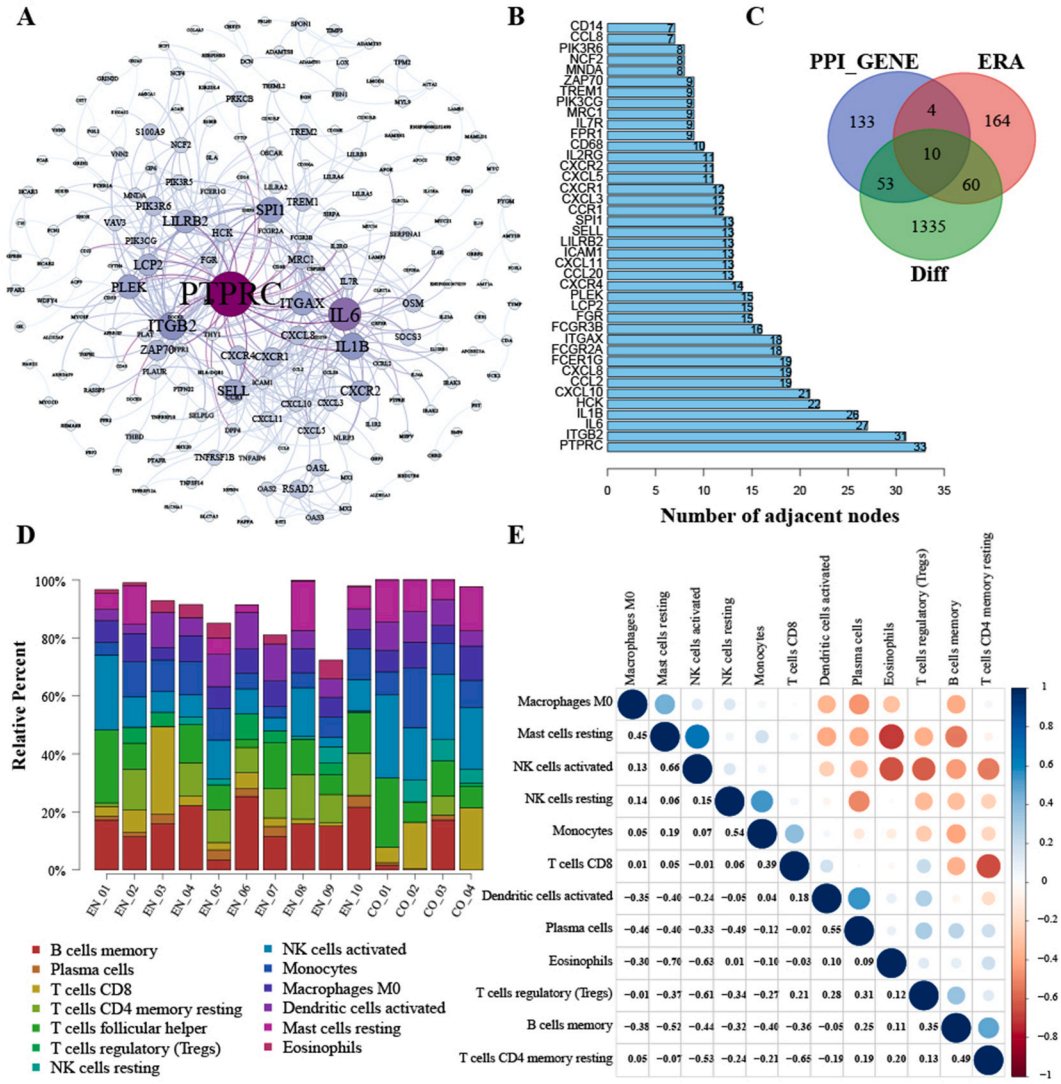

Fig. 4. Hub genes identification and immune-infiltration analysis of all samples. **A.** Protein-protein interaction (PPI) of the involved genes of iDEGs and sDEGs, where source nodes were linked with target nodes. **B.** Node genes identification by assessing their adjacent nodes. **C.** Hub genes shared by DEGs, 70 ERA-related DEGs, and node genes. **D.** Immune cell infiltration ratio of each sample. **E.** Correlation of the detected immune cells in all endometrial tissues, with colors and node sizes indicating the correlation coefficient. (For interpretation of the references to color in this figure legend, the reader is referred to the Web version of this article.)

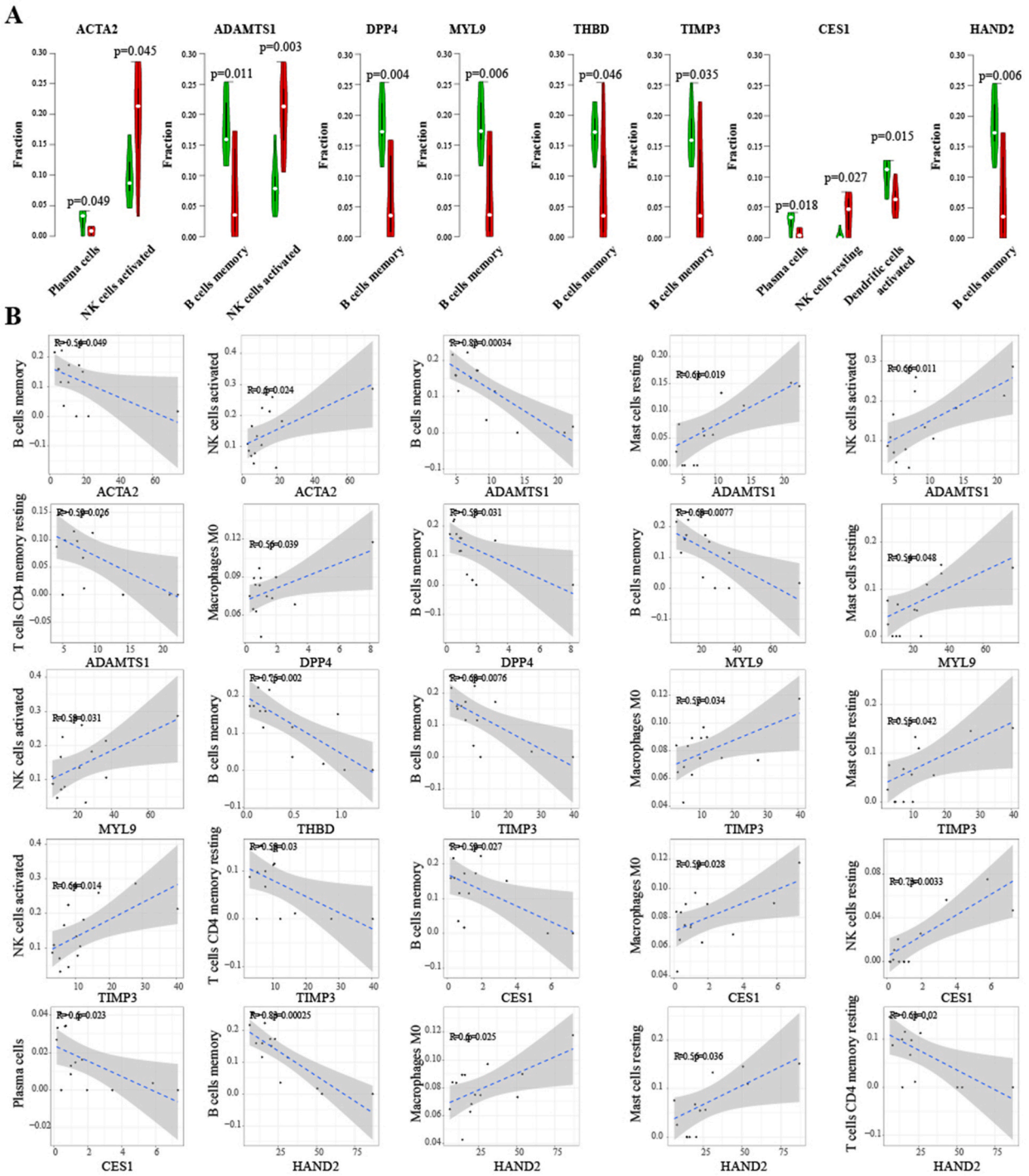

Fig. 5. Difference and correlation of immune-infiltration proportion with the expression of all hub genes. **A.** Differentially infiltrated immune cells grouped by the expression of traced hub genes by subgroup analysis. Violin plot showed the ratio differentiation of immune cells between samples with low or high gene expression, where Y-axis represented the proportion of immune cells. **B.** Correlation between the expression level of all hub genes and immune cells based on correlation analysis. Scatter plot here showed the correlation of immune cells proportion with the expression of genes. The red line in each plot was fitted with a linear model indicating the proportion tropism of the immune cells along with gene expression. X-axis indicated the expression level of target genes and Y-axis represented the proportion of immune cells. (For interpretation of the references to color in this figure legend, the reader is referred to the Web version of this article.)

cells, instead of Treg cells. What's more, the resting $CD4^+$ T memory cells shared a positive relationship with the activated NK cells and $CD8^+$ T cells but not the B memory cells (Fig. 4F).

3.7. Concerned immune cells determination

The difference and correlation analyses were performed to elucidate the modulatory landscape of the immune cell subsets affected by these hub genes. Our findings indicated that resting or activated NK cells were chiefly recruited in groups with higher expression of CES1.*ACTA2*, *ADAMTS1*, and *CES1*. Besides this, the memory B cells were down-regulated in groups when genes, including *ADAMTS1*, *DPP4*, *MYL9*, *THBD*, *TIMP3*, and *HAND2*, were up-regulated, as seen in Fig. 5A. When considering the expression correlation between hub genes and target immune cells, it was noticed that the memory B cells appeared to have negative regulatory relevance with the expression levels of *ACTA2*, *ADAMTS1*, *DPP4*, *MYL9*, *THBD*, *TIMP3*, *CES1*, and *HAND2*. On the contrary, the enrichment degree of the resting or activated NK cells was positively interrelated to *ACTA2*, *ADAMTS1*, *MYL9*, *TIMP3*, and *CES1*. Similarly, the infiltration extent of mast cells was also positively correlated with the expression of *ADAMTS1*, *MYL9*, *TIMP3*, and *HAND2*. (Fig. 5B). Based on the above findings, the intersection of the difference and correlation analyses was carried out. As observed in Fig. 6A–H, eight hub genes and three types of immune cells, including the resting or activated NK cells and memory B cells, were finally determined to be inseparable in the modulation of endometrial receptivity and tumor microenvironment.

4. Discussion

This research provided a whole landscape regarding the assisted reproduction outcomes of EC/EIN patients receiving fertility-sparing treatment in terms of the pathological character of the disease, endocrinological and metabolic status, IVF/ICSI parameters, and endometrial transcriptome. Even after achieving CR, the endometrial thickness and transcriptome at WOI were distinguished from normal controls. It is safe to assume EC/EIN and fertility-sparing therapy could leave a sequela on endometrial receptivity. The alternation of endometrial characteristics like decidualization and immune microenvironment after reversal of endometrium lesion may be responsible for the low pregnancy rate.

Reversal of EC/EIN lesions by progestin therapy, particularly with HESP, is believed to happen through the activation of

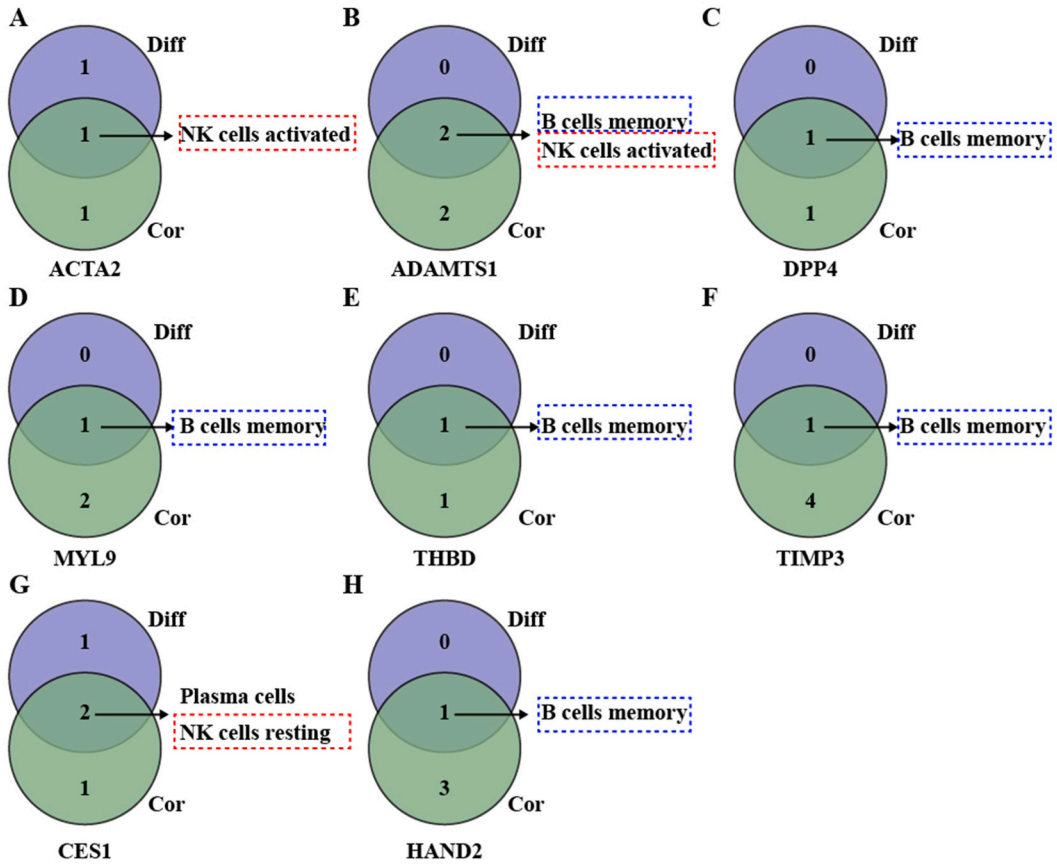

Fig. 6. Core immune cells exploration. **A-H.** Core immune cells were determined by difference and correlation analysis of the selected hub genes, as presented in the Venn plots, respectively.

progesterone receptors, leading to extensive stromal decidualization and subsequent atrophy of the endometrial epithelia [6]. All patients belong to p53-wild-type adenocarcinoma or atypical hyperplasia of the endometrium, and they have all reached CR of their EC/EIN. However, even with abundant embryos in IVF/ICSI, only half of these patients succeeded in pregnancy with ERA-guided frozen embryo transfer. The low implantation rate may result from the endometrial lesion itself, the medical treatment process, or repeated curettage. Besides, regarding metabolism, EC/EIN patients are prone to obesity and get glucose and lipid metabolic disorders [24]. These aspects could leave a detrimental effect on their normal endometrial function, even if all ten patients have been cured from the perspective of pathology. Therefore, comprehensive exploration should be conducted to answer why the sparing of the uterus does not equal the preservation of fertility.

The arrival of the transcriptome revolution brings us intensely scrutinized profiles of endometrium receptivity in WOI. The ERA was created as a customized array containing 238 genes coupled to a computational predictor, regardless of the endometrial histological appearance [22]. In terms of accuracy and reproducibility, these ERA-gene dating achieved a concordance of luteinising hormone peak, and the result can be reproduced 29–40 months later [23]. The WOI status by ERA of four cases (Cases 3, 5, 9 &10) from the EC/EIN group was tested to be pre-receptive (about 29–36 h earlier to receptive status), while the rest six cases and the whole control group all fell within the normal window. The published ERA computational algorithm classified non-receptive endometrium as 84 % pre- and 16 % post-receptive status [21]. All four cases with shifted WOI belonged to pre-receptive status as well, and we conducted personalized ET-postpone their ET opportunity guided by ERA results. However, only Case 3 got pregnant. Some retrospective cohorts have reached a similar conclusion that ERA cannot optimize the ET outcome in recurrent implantation failure cases, even with adjusted WOI, indicating that the low implantation rate is an attribute not only to shifted WOI but other endometrial factors [25,26]. 70 genes from the 238 ERA genes are also shared in the DGEs between the disease and control groups, which indicates that endometrial lesions would alter the endometrial receptivity. Since there are 1458 DEGs between EC/EIN patients and the control, other elements like neoplastic damage, immune microenvironment, or decidualization could affect the receptivity.

Besides, the receptivity transcriptomes of both groups are derived from bulk endometrial tissue. As a matter of fact, there are six main cell types identified in the endometrium: epithelial and endothelial cells, stromal fibroblasts, lymphocytes, macrophages, and a novel ciliated epithelial cell type [27]. Embryo implantation (trophoblast invasion) is a complex process involving interactions with glands, stromal cells, spiral arteries, and immune cells like uterine natural killer (uNK) cells [28]. This corresponds to the differential gene expression in our cases regarding ECM and immune-related signaling pathways, and the dysregulation in their cross-talk may account for the implantation failure after EC/EIN regression. Abundant immune cells reside in the endometrium and will be in close contact with the infiltrating embryos. With the opening of WOI, decidualization happens when a fundamental immune alteration occurs locally in the endometrium to avoid the rejection of a semi-allogenic embryo and promote its nutrition. During that time, adaptive immune cells should have escaped from the endometrium [29]; however, in our cohort, the EC/EIN patients had a significantly higher infiltration percentage of adaptive immune cells, particularly the memory B cells and memory $CD4^+$ T cells. This is opposite to the physiology of decidualization, likely owing to the previous tumor invasion and damage to the local microenvironment; the existing neoplasia stimulates adaptive immunity and left memory cells. These overactive adaptive immune cells may destroy the endometrium-embryo synchronization and eventually lead to the rejection of the embryo. On contrary to adaptive immunity, innate immune cells dash into the endometrium at WOI, and uNK cells account for 70 % of them [28]. The uNK cell differs from circulating NK cells by the cytokines they secrete and its low cytotoxic potential [30]. Their phenotype is $CD56^{hi}CD57^{lo}$ and attracted by IL-15 secreted by stroma cells in the decidua. It maintains immunological self-tolerance by preventing immune and autoimmune responses against self-antigens. The uNK cells generate cytokines related to the construction of the placenta and act on human leukocyte antigen-C to induce immune tolerance [30]. They are able to provide growth factors for trophoblast invasion and promote adaptations in the uterine vasculature [14]. The control group showed NK cells were the dominant subtype, and its number was much more abundant than the EC/EIN group. For robust pregnancy, decidual immune cells must be present with appropriate phenotypes to drive the remodelling of the endometrial vascular bed and stromal response. Therefore, EC/EIN-related tumor signals would change sex hormone-driven endometrial gene transcription and cell types and orgnization of the mucosal immunityduring the mid-luteal phase, impairing decidualization, endometrial immune microenvironment [31]. These deleterious variation from normal decidua account for the low receptivity in patients with EC/EIN after HESP treatment.

The main limitation of this work is the small sample size of the cohort. Only very limited cases received fertility-sparing treatment of EC/EIN followed IVF/ICSI procedure and were willing to donate endometrial samples exactly at the WOI stage, and so was the control group. However, this also reflects the high value of our work. In addition, we did not distinguish the different subtypes of NK cells in this research but only demonstrated that normal endometrium is significantly richer in NK cell infiltration. This result is in accordance with the endometrial immune characteristics at the WOI stage, the relatively higher level of NK cells in the control group than in the tumor group [31]. In our future exploration, uNK cells should be filtered from the bulk immune cells, and an *in-vitro* experiment will be conducted to test whether the uNK function has been compromised when co-cultured with decidua cells after CR of EC/EIN.

5. Conclusions

HESP is an effective therapy to reverse EC/EIN in histology in patients who fit the criteria for fertility-sparing treatment. In the following IVF/ICSI treatment, endometrial thickness and receptivity have been impaired, leading to a low implantation rate even with adjusted WOI. We compared the transcriptome of endometrial tissue at the WOI stage between patients after fertility-sparing treatment of EC/EIN and healthy young women. The 1458 DEGs were identified, and 70 belong to the ERA genes, which means they might have some association with endometrial receptivity. Further, the decidualization, particularly the endometrial immune microenvironment,

has been altered, as observed in this research, even after the CR of EC/EIN. The increased adaptive immune cells and decreased NK cell infiltration in the endometrium at the WOI stage may account for the damaged endometrial receptivity. Therefore, this work will offer a novel evaluation strategy on the fecundity of EC/EIN patients, which needs further validation by a larger sample size to make it more accurate.

Ethics approval and consent to participate

The study was conducted in accordance with the Declaration of Helsinki and approved by the Ethics Committee of Peking Union Medical College Hospital (JS-3329).

Consent for publication

Written informed consent has been obtained from all participants involved in the study to publish this paper.

Availability of data and materials

All data generated in this study have been presented in the manuscript or the supplementary files. The raw files of RNA sequencing have been uploaded to the public repository of NCBI and can be retrieved from the database (BioProject ID: PRJNA1018696 https://submit.ncbi.nlm.nih.gov/).

Funding

This work was supported by grants from Special Support Plan for Clinical Research in Central High-level Hospital of PUMCH (grant number 2022-PUMCH-A-230), Beijing Natural Science Foundation (grant number 7234411), the Non-profit Central Research Institute Fund of Chinese Academy of Medical Sciences (grant number 3332023008), China Postdoctoral Science Foundation (grant number 2023M740320) and the National High Level Hospital Clinical Research Funding (grant number 2022-PUMCH-B-123).

CRediT authorship contribution statement

Penghui Feng: Writing – review & editing, Writing – original draft, Software, Resources, Methodology, Investigation, Formal analysis, Data curation. **Duoduo Zhang:** Writing – review & editing, Writing – original draft, Software, Resources, Investigation, Formal analysis, Data curation. **Jingran Zhen:** Resources, Project administration, Methodology, Conceptualization. **Rong Chen:** Supervision, Resources, Project administration, Investigation, Conceptualization.

Declaration of competing interest

The authors declare that they have no known competing financial interests or personal relationships that could have appeared to influence the work reported in this paper.

Acknowledgements

We are grateful to all participants for supporting this study.

References

[1] H. Sung, et al., Global cancer statistics 2020: GLOBOCAN estimates of incidence and mortality worldwide for 36 cancers in 185 countries, CA A Cancer J. Clin. 71 (3) (2021) 209–249.
[2] F. Amant, et al., Endometrial cancer, Lancet 366 (9484) (2005) 491–505.
[3] Z. Fan, et al., Fertility-preserving treatment in young women with grade 1 presumed stage ia endometrial adenocarcinoma: a meta-analysis, Int. J. Gynecol. Cancer 28 (2) (2018) 385–393.
[4] N. Colombo, et al., ESMO-ESGO-ESTRO consensus conference on endometrial cancer: diagnosis, treatment and follow-up, Ann. Oncol. 27 (1) (2016) 16–41.
[5] J.J. Kim, et al., Role of progesterone in endometrial cancer, Semin. Reprod. Med. 28 (1) (2010) 81–90.
[6] C.C. Gunderson, et al., Oncologic and reproductive outcomes with progestin therapy in women with endometrial hyperplasia and grade 1 adenocarcinoma: a systematic review, Gynecol. Oncol. 125 (2) (2012) 477–482.
[7] C.D. Duoduo Zhang, Yu Qi, Lingya Pan, Hanbi Wang, Clinical analysis of infertility patients undergoing in vitro fertilization with a levonorgestrel intrauterine system in situ after conservative treatment of early well-differentiated endometrial adenocarcinoma and atypical endometrial hyperplasia, Chinese Journal of Reproduction and Contraception 41 (3) (2021) 237–241 (in Chinese).
[8] S. Tamauchi, et al., Efficacy of medroxyprogesterone acetate treatment and retreatment for atypical endometrial hyperplasia and endometrial cancer, J. Obstet. Gynaecol. Res. 44 (1) (2018) 151–156.
[9] W. Yamagami, et al., Is repeated high-dose medroxyprogesterone acetate (MPA) therapy permissible for patients with early stage endometrial cancer or atypical endometrial hyperplasia who desire preserving fertility? J Gynecol Oncol 29 (2) (2018) e21.
[10] J. Wei, et al., Comparison of fertility-sparing treatments in patients with early endometrial cancer and atypical complex hyperplasia: a meta-analysis and systematic review, Medicine (Baltim.) 96 (37) (2017) e8034.
[11] M.F. Freedman, et al., Avoiding Asherman's syndrome: refining our approach to uterine evacuation, Fertil. Steril. 116 (4) (2021) 961–962.
[12] B.A. Lessey, et al., What exactly is endometrial receptivity? Fertil. Steril. 111 (4) (2019) 611–617.

[13] C. Chan, et al., Discovery of biomarkers of endometrial receptivity through a minimally invasive approach: a validation study with implications for assisted reproduction, Fertil. Steril. 100 (3) (2013) 810–817.
[14] S.A. Robertson, et al., Immune determinants of endometrial receptivity: a biological perspective, Fertil. Steril. 117 (6) (2022) 1107–1120.
[15] G. Yu, et al., clusterProfiler: an R package for comparing biological themes among gene clusters, OMICS 16 (5) (2012) 284–287.
[16] S. Hanzelmann, et al., GSVA: gene set variation analysis for microarray and RNA-seq data, BMC Bioinf. 14 (2013) 7.
[17] D. Szklarczyk, et al., The STRING database in 2021: customizable protein-protein networks, and functional characterization of user-uploaded gene/measurement sets, Nucleic Acids Res. 49 (D1) (2021) D605–D612.
[18] K. Yoshihara, et al., Inferring tumour purity and stromal and immune cell admixture from expression data, Nat. Commun. 4 (2013) 2612.
[19] M.E. Ritchie, et al., Limma powers differential expression analyses for RNA-sequencing and microarray studies, Nucleic Acids Res. 43 (7) (2015) e47.
[20] Q. Tang, et al., Optimal cut-off values for the homeostasis model assessment of insulin resistance (HOMA-IR) and pre-diabetes screening: developments in research and prospects for the future, Drug Discov Ther 9 (6) (2015) 380–385.
[21] M. Ruiz-Alonso, et al., The endometrial receptivity array for diagnosis and personalized embryo transfer as a treatment for patients with repeated implantation failure, Fertil. Steril. 100 (3) (2013) 818–824.
[22] P. Diaz-Gimeno, et al., A genomic diagnostic tool for human endometrial receptivity based on the transcriptomic signature, Fertil. Steril. 95 (1) (2011) 50–60.
[23] M. Ruiz-Alonso, et al., Endometrial receptivity analysis (ERA): data versus opinions, Hum Reprod Open 2021 (2) (2021) hoab011.
[24] A. Talhouk, et al., Confirmation of ProMisE: a simple, genomics-based clinical classifier for endometrial cancer, Cancer 123 (5) (2017) 802–813.
[25] J. Tan, et al., The role of the endometrial receptivity array (ERA) in patients who have failed euploid embryo transfers, J. Assist. Reprod. Genet. 35 (4) (2018) 683–692.
[26] J.A. Patel, et al., Personalized embryo transfer helps in improving in vitro fertilization/ICSI outcomes in patients with recurrent implantation failure, J. Hum. Reprod. Sci. 12 (1) (2019) 59–66.
[27] W. Wang, et al., Single-cell transcriptomic atlas of the human endometrium during the menstrual cycle, Nat. Med. 26 (10) (2020) 1644–1653.
[28] J.M. Franasiak, et al., A review of the pathophysiology of recurrent implantation failure, Fertil. Steril. 116 (6) (2021) 1436–1448.
[29] S. Sakaguchi, et al., Regulatory T cells and immune tolerance, Cell 133 (5) (2008) 775–787.
[30] A. Moffett, et al., Uterine NK cells: active regulators at the maternal-fetal interface, J. Clin. Invest. 124 (5) (2014) 1872–1879.
[31] N. Ledee, et al., Endometrial immune profiling: a method to design personalized care in assisted reproductive medicine, Front. Immunol. 11 (2020) 1032.